Development of Prosthesis Grasp Control Systems on a Robotic Testbed

Bart Peerdeman[*], Ugo Fabrizi[†], Gianluca Palli[†], Claudio Melchiorri[†], Stefano Stramigioli[*], and Sarthak Misra[*]

Abstract— **Modern myoelectric hand prostheses continue to increase in functionality, while their control is constrained by the limits of myoelectric input. This paper covers the development and testing of grasp control systems for multifunctional myoelectric prosthetic hands. The functionality of modern hand prostheses is often focused on the task of grasping, which can be divided into high-level grasp planning and low-level finger control. Initially, models can used to test these control systems, but for proper evaluation actual implementation on a physical system is required. The University of Bologna (UB) Hand IV prototype is an anthropomorphic, tendon-driven robotic hand, which makes it well-suited to represent the structure of modern prostheses. One of the main control systems tested in this paper is based on the intrinsically passive controller (IPC), the structure of which offers guaranteed passivity and stability. After several grasping tests, the systems are evaluated on compliant behavior, grasping ability, and dynamic appearance. IPC proves to be a powerful approach to interaction control, without the associated sensor requirements which could be difficult to meet in modern hand prostheses.**

I. INTRODUCTION

Unilateral amputees often use their sound hand to perform single-handed tasks. During bi-manual activities, the sound hand is used to manipulate objects while a prosthesis is used for support, which mostly involves the grasping and holding of objects. Current commercially available myoelectric prostheses [1], [2], [3] and recently developed prosthesis prototypes [4], [5], [6] are becoming increasingly anthropomorphic, with a high number of degrees of freedom (DOF). To effectively use this increased functionality while still remaining intuitive to the user, new grasp control systems are required. Such a system needs to provide a small but versatile selection of distinct grasp types (Figure 1), which can be operated with simple myoelectric commands for grasp selection, opening and closing. The grasp controller itself will then determine the right finger positions and orientations. Once the target positions have been determined, the fingers also need to be properly controlled to their end position. Since the hand has to interact with an unknown environment while remaining sufficiently safe for human interaction, this control needs to be both compliant and robust [7].

Basic position or force control systems respond badly to interaction with the environment [8]. To remedy this, several variations of interaction control have been developed, which

(a)   (b)   (c)
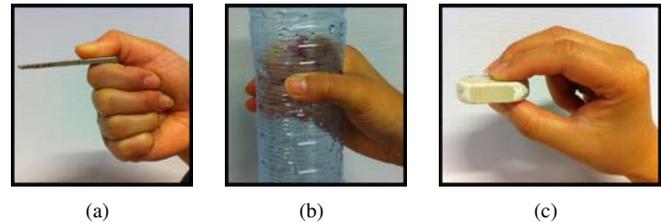
Fig. 1. Illustration of the different grasp types to be analyzed: (a) The lateral grasp; flexing all fingers and using the thumb to grasp flat objects. (b) The cylindrical grasp; surrounding an object with all fingers and the thumb. (c) The tripod grasp; using the index finger, middle finger and thumb to pick up small objects.

seek to establish a dynamic relationship with the environment. While this improves these systems' ability to handle contact, they often require additional information about the system or its environment. The intrinsically passive controller (IPC) [8] provides an alternative to these types of interaction control. It consists of virtual springs exerting forces on the fingertips of the hand; these springs are connected to each other by a virtual object, which serves as the focus of the grasp. An advantage of this system is that it only requires fingertip position information.

The combination of IPC with a high-level grasp planner allows a multifunctional prosthesis to perform a variety of compliant grasps, while remaining intuitively controllable with only few myoelectric input signals.

In this paper, the viability of the IPC system for prosthetic grasp control is evaluated in comparison to position, admittance, and impedance control. Initially a bio-mechanical model of the hand [9] is used for testing the interaction controllers; the IPC controller then is implemented on the University of Bologna's (UB) robotic hand, the UB Hand IV. Though not a prosthesis itself, the UB Hand IV is used as a testbed for the control of hand prostheses because of its anthropomorphic design and high number of DOF.

This paper is organized as follows: in Section 2, the design choices and features of the UB Hand IV are described. Section 3 covers the various control systems and their components. In Section 4, the control system parameters are derived, and the experimental protocol is explained. Section 5 describes the experimental results. We conclude in Section 6, and the results and directions for future work are discussed.

II. UB HAND IV DESIGN

Current robotic hands are mainly designed based on conventional mechanics and robotics. Alternatively, the human hand can inspire an innovative robotic hand design. This approach has been adopted within the DEXMART project
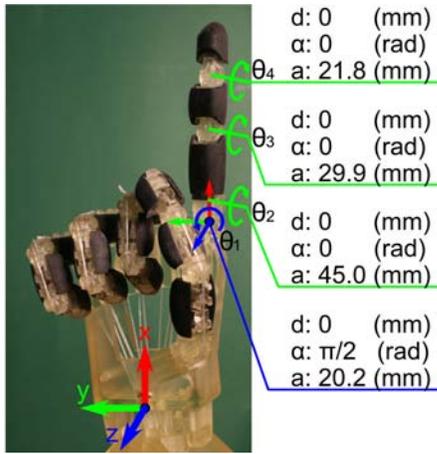
Fig. 2. A diagram illustrating the UB Hand IV's wrist base frame, index finger base frame, and the Denavit-Hartenberg parameters of the fingers.

[10] for the development of the UB Hand IV. In this section, the main features of the hand's anthropomorphic design are discussed.

A. Parameters

The UB Hand IV possesses a total of 20 independent DOF, divided across 5 identical fingers. Each finger has three flexion/extension DOF, with one adduction/abduction DOF in the proximal joint. The distal flexion joint of each finger is passive; it is coupled to the middle flexion joint by an internal tendon.

The Denavit-Hartenberg parameters of the fingers are shown in Figure 2. The joint angles of each finger are mechanically constrained to the following intervals:

$$\theta_1 \in [-\pi/18, \, \pi/18] \text{ and } \theta_{\{2,3,4\}} \in [0, \, \pi/2] \quad \text{(rad)} \quad (1)$$

B. Endoskeletal structure

The endoskeletal design of the UB Hand's fingers allows sufficient room in the hand for sensors and related electronics. However, the complex shapes of the links are difficult to manufacture conventionally. Therefore, an additive manufacture technology (fused deposition modeling) has been implemented. Currently, integrated pin joints are used to connect the phalanges [11]; the design of these joints can be seen in Figure 3.

C. Tendon-based transmission

As current technology does not allow the placement of more than a few actuators in an anthropomorphic robotic hand, it is necessary to place the actuators remotely, and use tendons for force transmission. Various tendon configurations have been proposed in literature [12], [13]. For the UB Hand IV, an 'N + 1' tendon configuration has been adopted, which can be seen in Figure 3. In this configuration, each joint DOF is actuated by a separate flexion tendon, with a single communal tendon for extension. It allows control of all joint DOF with a minimal number of actuators, and without any pretension mechanisms.
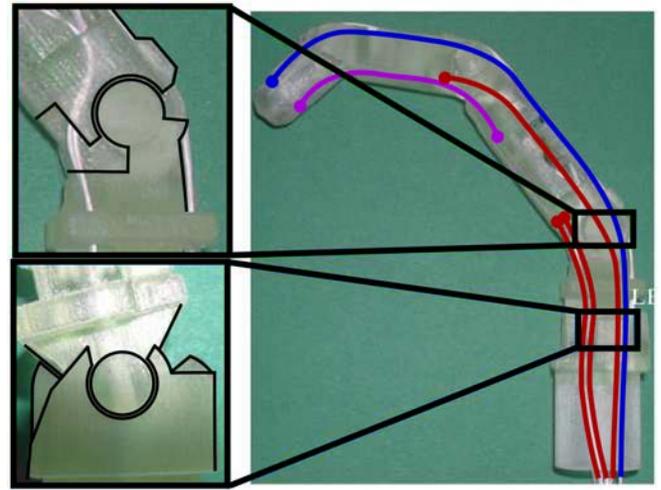
Fig. 3. A close-up view of the UB Hand IV's integrated pin joints, as well as its internal tendon paths. Flexion tendons are marked in red, the extension tendon is blue, and the passive tendon is marked in purple.

Routing the tendons from the motors to the joints is often done via pulleys attached to the joints, which is mechanically complicated. In the UB Hand, the tendons are routed through canals within the endoskeletal structure of the phalanges. The use of these tendon canals is a convenient solution due to its simplicity, though it introduces distributed friction along the tendon, which needs to be accounted for [14], [15]. A complete description of the UB Hand IV finger kinematics and tendon network can be found in [16].

D. Control

The hardware used to control the UB Hand IV can be seen in Figure 4. Since the I/O board does not possess a sufficient number of input and output channels, two interfacing boards for the multiplexing/demultiplexing of the signals have been built. The controllers are developed in a Matlab/Simulink [17] environment on a separate PC, using the Matlab Real-Time Workshop toolbox.

As modern hand prostheses continue to increase in both anthropomorphism and DOF, the UB Hand's design makes it a fitting testbed for the control of future hand prostheses.

III. CONTROL SYSTEM STRUCTURE

To provide an intuitive way of governing the complex motions of all the prosthesis' joints, the control system is organized hierarchically. Based on myoelectric input signals from the user, a high-level grasp planner provides target behaviors for the low-level controller, which governs the individual fingers. Various possible implementations of these systems, and their advantages and disadvantages, are discussed in this section.

A. High-level control: grasp planning

To allow the user to easily perform a grasp, the grasping process has to be divided into several discrete stages, which
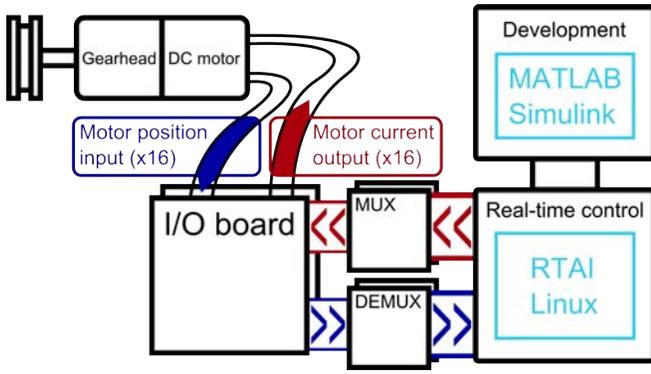
Fig. 4. A block diagram describing the UB Hand IV control hardware. For actuation, commercial DC motors with integrated speed reducers and absolute encoders are used. The I/O board is a Sensoray 626 PCI analog and digital I/O card. The real-time control PC is a Pentium 4 at 1.8 GHz running the RTAI Linux operating system [18].

Fig. 5. The various components of the IPC. Virtual springs (blue) with stiffness ($\mathbf{K}$) connect the virtual object ($\mathbf{M_v}$) to the fingertips ($\mathbf{M}$). The virtual object is connected by another spring ($\mathbf{K_v}$) to the virtual end position (red). A damper ($\mathbf{b}$) is also connected to the virtual object. On the right, a detailed view of a virtual spring is shown, with variable endpoint frames Ψ_i and Ψ_j.

can be switched between by means of input signals. In general, two stages can be defined: preshaping and grasp execution. Once a grasp type has been selected, the grasp is preshaped by moving the fingers to the correct starting position for that grasp. Grasp execution involves the automatic closing of the grasp around an object, the degree to which can be controlled by the user.

According to the requirements analysis performed in [7], three important grasp types for daily activities are the lateral, tripod, and cylindrical grasps. The end positions of these grasps are shown in Figure 1.

The lateral grasp (Figure 1(a)) can be used for grasping flat objects securely. Preshaping is performed by fully flexing the index through little fingers, with grasp execution consisting of flexion of the fully unopposed thumb.

The cylindrical grasp (Figure 1(b)), for powerfully grasping larger objects, is preshaped by fully opposing the thumb and executed by flexing the thumb shortly after starting to flex all other fingers simultaneously.

The tripod grasp (Figure 1(c)) is a precise grasp used to pick up small objects. It is preshaped by opposing the thumb to the index and middle fingers, and fully flexing the little and ring fingers. Grasp execution consists of flexion of the index finger, middle finger and thumb.

To control a grasp with this system, only five input signals need to be distinguished; three for selecting the grasp type, and two for opening and closing the grasp.

B. Low-level control systems

These control systems calculate the desired wrench to be applied to each fingertip ($\mathbf{W}_{EE}$), which is converted into torques on the individual joints of the finger using the Jacobian ($\mathbf{J}(\theta)$):

$$\boldsymbol{\tau}_{joints} = \mathbf{J}(\theta)^T \mathbf{W}_{EE} \qquad (2)$$

The desired joint torques are then converted to actuator torques by the UB Hand IV's torque controller [16].

1) Proportional control: The most basic method of control used here is a Cartesian proportional control system. It applies a fingertip force linearly dependent on the distance from the fingertip position ($\mathbf{x}$) to the target ($\mathbf{x}_d$), defined by the gain value ($\mathbf{K}$):

$$\mathbf{W}_{EE} = \mathbf{K}(\mathbf{x}_d - \mathbf{x}) \qquad (3)$$

Proportional control is easy to implement, but is not a valid method of handling interaction [19]. Therefore, the use of this type of control system is limited to preshaping the hand or performing free space motion.

2) Interaction control: To make a control system more robust to contact, it can be designed to control the dynamic interaction with the environment. Several possible approaches are available, all of which establish a relation between internal/external forces and positions/velocities of the fingers.

One way of approaching this is admittance control. It involves implementing a basic proportional controller, and changing its reference position based on external forces. The relationship between the measured external forces ($\mathbf{F}_{ext}$) and target/reference positions ($\mathbf{x}_d/\mathbf{x}_r$) is modeled as a mechanical admittance, with inertia ($\mathbf{M}$), damping ($\mathbf{D}$), and stiffness ($\mathbf{K}$):

$$\mathbf{M}\ddot{\mathbf{x}}_r + \mathbf{D}(\dot{\mathbf{x}}_r - \dot{\mathbf{x}}_d) + \mathbf{K}(\mathbf{x}_r - \mathbf{x}_d) = \mathbf{F}_{ext} \qquad (4)$$

The resulting new reference position ($\mathbf{x}_r$) is then entered into the proportional controller (3) instead of the previous target ($\mathbf{x}_d$) to calculate the fingertip wrench to be applied.

In [19], it is argued that the environment of any manipulator can best be described as an admittance, and that for proper dynamic interaction the manipulator should behave like its complement, an impedance. In impedance control, the difference between the fingertip's current state (position, orientation, and their derivatives) and that of the target determine the wrench to be applied. In this case, its implementation is similar to a spring-damper system:

$$\mathbf{W}_{EE} = \mathbf{D}(\dot{\mathbf{x}}_d - \dot{\mathbf{x}}) + \mathbf{K}(\mathbf{x}_d - \mathbf{x}) \qquad (5)$$
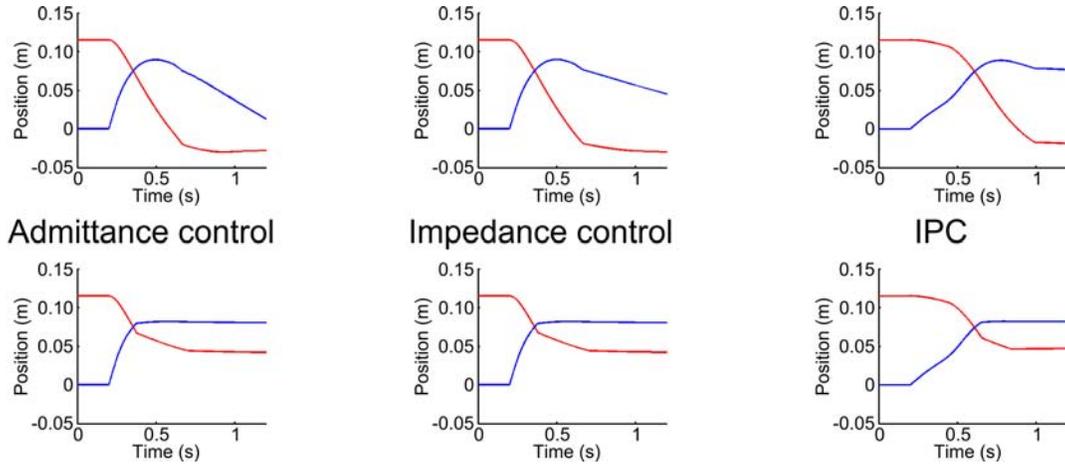
Fig. 6. Simulation results for cylinder grasp testing on the UB Hand model in free space (above) and with an object (below). The index fingertip x position is shown in red, and its z position in blue (see Figure 2 for the finger base frame).

Alternatively, this control can also be located in the joints themselves, establishing a direct relation between the current and desired joint angles/velocities, and the joint torques [20].

It should be noted that the mentioned interaction control systems may require more advanced information on the system, such as external forces and velocities. While improving the dynamic behavior, these added requirements can be restrictive.

3) Intrinsically Passive Control (IPC): This control method [8] establishes virtual springs between the fingertips and a virtual object, the dynamics of which are modeled in the controller. The virtual object is the center of the grasp, and is connected via another spring to a virtual end position. A diagram representing this controller can be seen in Figure 5. The virtual springs, shown in Figure 5, exert wrenches ($\mathbf{W}$) on their end points i and j, with coordinate frames Ψ_i and Ψ_j, respectively. These wrenches consist of torque ($\mathbf{m}$) and force ($\mathbf{f}$) components, and are based on the differences in orientation ($\mathbf{R}_j^i$) and position ($\mathbf{p}_i^j$) of the endpoints as follows [8]:

$$\mathbf{W}_i = \left[\begin{array}{c} \mathbf{m}_i \\ \mathbf{f}_i \end{array} \right] \qquad (6)$$

$$\tilde{\mathbf{m}}_i = -2(\mathbf{G}_o\mathbf{R}_i^j)_A - (\mathbf{G}_t\mathbf{R}_j^i\tilde{\mathbf{p}}_i^j\tilde{\mathbf{p}}_i^j\mathbf{R}_i^j)_A - 2(\mathbf{G}_c\tilde{\mathbf{p}}_i^j\mathbf{R}_i^j)_A \quad (7)$$

$$\tilde{\mathbf{f}}_i = -\mathbf{R}_j^i(\mathbf{G}_t\tilde{\mathbf{p}}_i^j)_A\mathbf{R}_i^j - (\mathbf{G}_t\mathbf{R}_j^i\tilde{\mathbf{p}}_i^j\mathbf{R}_i^j)_A - 2(\mathbf{G}_c\mathbf{R}_i^j)_A \quad (8)$$

$\tilde{}$ represents the twist operation, and $()_A$ determines the antisymmetric part of the matrix. These torques and forces are based on translational ($\mathbf{G}_t$), orientational ($\mathbf{G}_o$) and coupling ($\mathbf{G}_c$) co-stiffnesses, which can be calculated from regular stiffness matrices ($\mathbf{K}_t, \mathbf{K}_o, \mathbf{K}_c$) as follows:

$$\mathbf{G}_* = \frac{1}{2}\text{Tr}(\mathbf{K}_*)(\mathbf{I} - \mathbf{K}_*) \qquad (9)$$

where $* = t, o, c$ and $\mathbf{I}$ is a 3×3 identity matrix. These stiffnesses can be changed in order to control the applied force. Additionally, the springs' rest length can be controlled by changing their connection points [21].

A damping force is applied to the virtual object, which guarantees the asymptotic stability of the system [8]. As the virtual object's state is fully observable, the implementation of damping can be done without requiring additional sensors. The points on the virtual object where the virtual springs are connected can be chosen in such a way as to surround an object with the fingers, which improves grasp performance. The grasp planner can control the system's dynamic behavior through manipulation of the virtual spring parameters and the location of the virtual end position.

IV. EXPERIMENT DESIGN

Before implementing and evaluating the different controller types, the appropriate parameters and setpoints should be determined. Afterward, the test protocol for simulation and UB Hand experimentation is described.

A. Controller parameters

The main parameters governing the interaction controllers' behavior are the damping ($\mathbf{D}$) and stiffness ($\mathbf{K}$) gains, which are chosen with regard to the maximum force that the hand's motors can continuously provide. In the UB Hand's case, this is approximately 50 N. The stiffness value is set accordingly, and the damping value is then tuned experimentally.

Relevant parameters for the IPC (Figure 5) include the inertial parameters of the virtual object ($\mathbf{M_v}$), the damping coefficient ($\mathbf{b}$), and the stiffnesses of the virtual springs ($\mathbf{K}$, $\mathbf{K_v}$). The virtual springs' stiffness values can be determined in the same way as with the interaction controllers. To make sure the higher-order system created by the application of damping directly on the virtual object resembles a basic second-order system as closely as possible, two limits are placed on the parameters: the mass of the virtual object should be lower than the mass of the rest of the system, and the spring connecting the virtual object to the virtual end position should be more compliant than those connecting the virtual object to the fingertips [22]. Additionally, to achieve critical damping, the damping coefficient ($\mathbf{b}$) should be determined as follows:
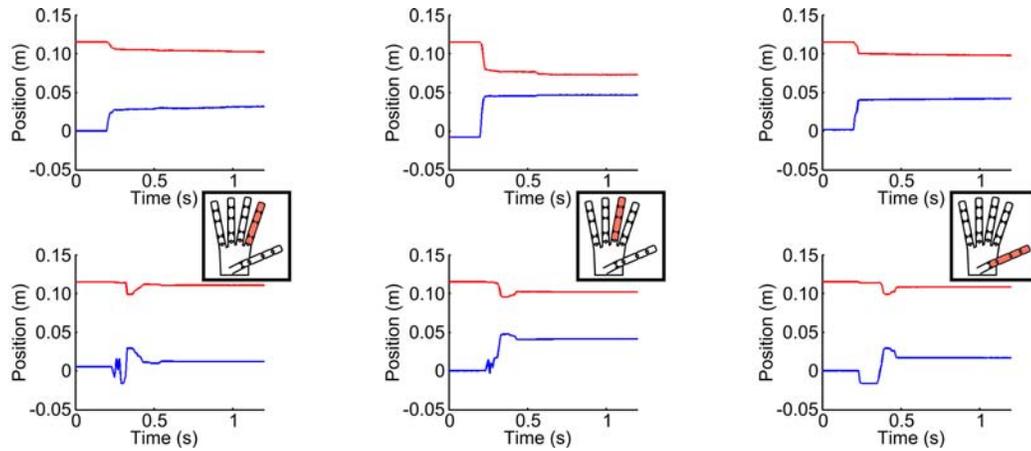
Fig. 7. Experimental results for free-space tripod grasping with the proportional controller (above) and IPC (below), implemented on the UB Hand IV. The fingertip x position is shown in red, and its z position in blue (see Figure 2 for the finger base frame).

$$\mathbf{b} = \mathbf{I} \cdot \sqrt{K_v M} \qquad (10)$$

where (K_v) is the (scalar) stiffness of the spring connecting the virtual object to the virtual end position and (M) represents the weight of the finger.

B. Grasp planning

Depending on the grasp type, the interaction control grasp planner assigns preshaping and grasping setpoints for each finger; these can be switched between by the user. To move the fingertips across a naturally curling trajectory, a path planner is implemented, using polar interpolation between the current fingertip position and the desired end point.

The IPC grasp planner determines two main parameters based on the grasp type: the location of the virtual end position (which influences the virtual object's location), and the location of the virtual spring end points, which represent the desired end configuration of the fingertips. Additionally, fingers that are not participating in the grasp are set to full flexion, and are not connected to the virtual object. For preshaping, the virtual springs' rest length is set to a high value, surrounding the virtual object with the fingertips and allowing the user to position the hand around the target. To close the grasp, the rest lengths are gradually reduced. During grasping, any obstruction of the fingers' movement will result in displacement of the virtual object, and the grasp focus will shift accordingly. This allows the hand to adapt to varying object shapes and motions, increasing the stability of the grasp.

C. Test protocol

As the current UB Hand hardware does not have sensors capable of determining joint velocity or external forces, the tested impedance and admittance controllers could not be implemented on it. Therefore, initial testing and evaluation of all controllers is done on a dynamic model of the UB Hand [9], implemented in Simulink [17]. In this simulation, the controllers are used to perform grasping motions with and without a simulated obstruction. After initial evaluation,

the IPC system is transferred to the UB Hand hardware. It is then used to execute the three grasp types shown in Figure 1 with and without an object.

V. RESULTS

The performance of the controllers was evaluated both in simulation and actual experiments on the UB Hand. The simulations and grasp trials all lasted for 1.2 seconds, with the controller changing from preshaping to closing at $t = 0.2$ s. The results of the simulation tests can be seen in Figure 6.

During free-space grasping, the IPC transferred from preshaping to grasping without discontinuity, while the interaction controllers exhibited a sudden start of motion. This did result in a response time delay of 0.1 s for the IPC. After the initial simulation tests, a cylindrical object was added to the model. While all controllers handled contact with the object well, the IPC reached its equilibrium position sooner than the interaction controllers.

Testing on the UB Hand IV was performed using IPC, as well as a proportional controller already present on the system. The results of these tests are shown in Figures 7 and 8. During free-space grasping the IPC showed some oscillations before arriving at a stable position, whereas the proportional controller moved directly to the target position.

The compliant behavior of the IPC during grasping resulted in a stable grasp; for example, when the thumb's limited abduction angle did not allow it to move to the virtual object's position, this caused the virtual object to shift accordingly, moving the grasp focus and completing the grasp. The proportional controller did not perform as well in this scenario, stopping before the fingers fully surrounded the object and not accommodating the object's motion.

VI. CONCLUSIONS AND FUTURE WORK

To compensate for the increased number of DOF in modern myoelectric prosthetic hands, advanced hierarchical control systems are necessary. The system developed here contains a global grasp planner, which sends setpoints to low-level finger controllers. This paper features the UB Hand IV, an anthropomorphic robotic hand developed by
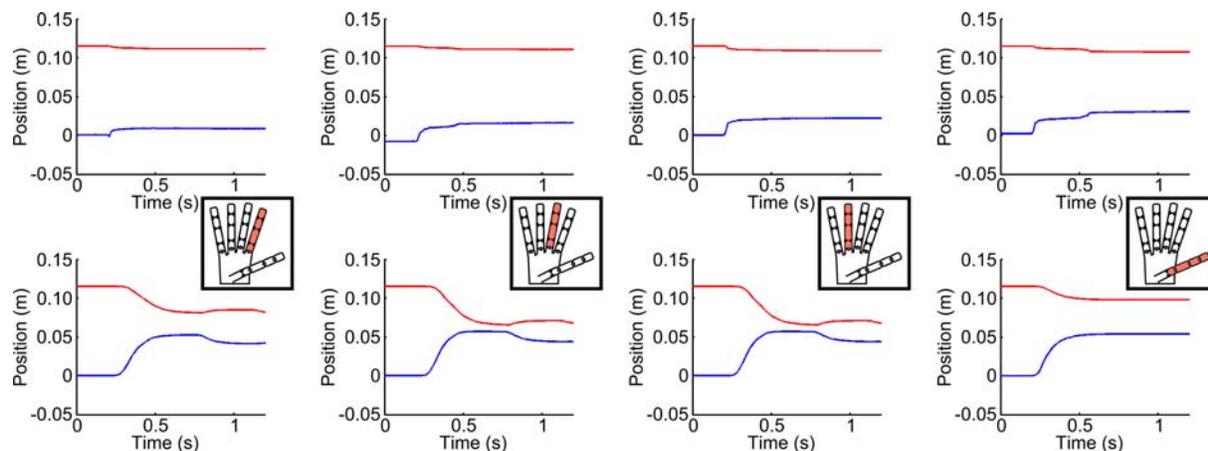
Fig. 8. Experimental results for cylinder grasping of an object with the proportional controller (above) and IPC (below), implemented on the UB Hand IV. The fingertip x position is shown in red, and its z position in blue (see Figure 2 for the finger base frame).

the University of Bologna using a three-dimensional printing process. It is used as a testbed for the development of prosthetic hand controllers; given the increase in DOF of modern prosthetic hands, control systems tested on the UB Hand IV can be considered suitable for implementation in future hand prostheses. After evaluating several types of interaction control, IPC was selected for testing, as it provides compliant control while working with only joint position information. This makes it useful for the control of prosthetic hands, which often interact with the environment and have tight constraints on available space and weight.

IPC has been implemented and tested on the UB Hand IV, performing three basic grasp types that represent activities of daily living. The results show that the IPC system is able to compliantly grasp a variety of objects and capable of dynamically adapting the focus of the grasp.

In future work, the development of a multifunctional prosthesis prototype with joint-mounted Hall sensors for angular position and force sensors in the fingertips would allow for the evaluation of IPC and interaction control systems in a practical setting. Additionally, real-time myoelectric input signals from test subjects can be used for evaluation of the high-level control system.

REFERENCES

[1] Touch Bionics Inc. i-LIMB Hand. http://www.touchbionics.com/i-LIMB.
[2] Otto Bock. Michelangelo Hand. http://www.ottobock.com/.
[3] RSLSteeper. bebionic. http://www.bebionic.com/.
[4] J. Pons, E. Rocon, R. Ceres, D. Reynaerts, B. Saro, S. Levin, and W. van Moorleghem, "The MANUS-HAND dextrous robotics upper limb prosthesis: Mechanical and manipulation aspects," *Autonomous Robots*, vol. 16, no. 2, pp. 143–163, 2004.
[5] S. Schulz, C. Pylatiuk, M. Reischl, J. Martin, R. Mikut, and G. Bretthauer, "A hydraulically driven multifunctional prosthetic hand," *Robotica*, vol. 23, no. 3, pp. 293–299, 2005.
[6] C. Cipriani, M. Controzzi, and M. C. Carrozza, "Progress towards the development of the smarthand transradial prosthesis," in *Proceedings of the IEEE International Conference on Rehabilitation Robotics (ICORR)*, Kyoto, Japan, June 2009, pp. 682–687.
[7] B. Peerdeman, D. Boere, H. Witteveen, R. Huis in 't Veld, H. Hermens, S. Stramigioli, J. Rietman, P. Veltink, and S. Misra, "Myoelectric forearm prostheses: State of the art from a user requirements perspective," *Journal of Rehabilitation Research & Development (JRRD)*, vol. 48, no. 6, pp. 719–738, July 2011.

[8] S. Stramigioli, *Modeling and IPC Control of Interactive Mechanical Systems: A Coordinate-Free Approach*. Springer-Verlag New York, Inc., 2001.
[9] B. Peerdeman, D. Boere, L. Kallenberg, S. Stramigioli, and S. Misra, "A modeling framework for control of myoelectric hand prostheses," in *Proceedings of the 32rd Annual International Conference of the IEEE Engineering in Medicine and Biology Society (EMBC)*, Buenos Aires, Argentina, September 2010, pp. 519–523.
[10] "DEXMART Project website," http://www.dexmart.eu/.
[11] L. Biagiotti, F. Lotti, C. Melchiorri, G. Palli, P. Tiezzi, and G. Vassura, "Development of UB Hand 3: Early results," in *Proceedings of the IEEE International Conference on Robotics and Automation (ICRA)*, Barcelona, Spain, April 2005, pp. 4488–4493.
[12] A. Bicchi and D. Prattichizzo, "Analysis and optimization of tendineous actuation for biomorphically designed robotic systems," *Robotica*, vol. 18, pp. 23–31, 2000.
[13] L. Barbieri and M. Bergamasco, "Nets of tendons and actuators: an anthropomorphic model for the actuation system of dexterous robot hands," in *Proceedings of the International Conference on Advanced Robotics (ICAR)*, Pisa, Italy, June 1991, pp. 357–362.
[14] M. Kaneko, M. Wada, H. Maekawa, and K. Tanie, "A new consideration on tendon-tension control system of robot hands," in *Proceedings of the IEEE International Conference on Robotics and Automation (ICRA)*, Sacramento, USA, April 1991, pp. 1028–1033.
[15] G. Palli, G. Borghesan, and C. Melchiorri, "Tendon-based transmission systems for robotic devices: Models and control algorithms," in *Proceedings of the IEEE International Conference on Robotics and Automation (ICRA)*, Kobe, Japan, May 2009, pp. 4063–4068.
[16] G. Borghesan, G. Palli, and C. Melchiorri, "Design of tendon-driven robotic fingers: Modeling and control issues," in *Proceedings of the IEEE International Conference on Robotics and Automation (ICRA)*, Anchorage, Alaska, May 2010, pp. 793–798.
[17] MATLAB, *version 7.10.0 (R2010a)*. The MathWorks Inc.: Natick, Massachusetts, 2010.
[18] E. Bianchi, L. Dozio, and P. Mantegazza, *A Hard Real Time support for LINUX*, Dipartimento di Ingegneria Aerospaziale, Politecnico di Milano, www.rtai.org.
[19] N. Hogan, "Impedance control: an approach to manipulation," *Journal of Dynamic Systems Measurement and Control*, vol. 107, pp. 1–24, 1985.
[20] L. Biagiotti, H. Liu, G. Hirzinger, and C. Melchiorri, "Cartesian impedance control for dexterous manipulation," in *Proceedings of the IEEE/RSJ International Conference on Intelligent Robots and Systems (IROS)*, Las Vegas, USA, October 2003, pp. 3270 – 3275.
[21] C. Secchi, S. Stramigioli, and C. Melchiorri, "Geometric grasping and telemanipulation," in *Proceedings of the IEEE/RSJ International Conference on Intelligent Robots and Systems*, Maui, USA, 2001, pp. 1763–1768.
[22] S. Stramigioli, "Creating artificial damping by means of damping injection," in *Proceedings of the ASME Dynamic Systems and Control Division*, Munich, Germany, 1996, pp. 601–606.